AD-A257 594

RL-TR-92-218
Final Technical Report
August 1992

AN OPTICAL CONSENSUS CORRELATOR FOR CLUTTERED TARGETS

Aerodyne Research Inc.

Dr. Roger S. Putnam

DTIC
ELECTE
NOV 24 1992
S B D

92-30077

APPROVED FOR PUBLIC RELEASE; DISTRIBUTION UNLIMITED.

Rome Laboratory
Air Force Systems Command
Griffiss Air Force Base, NY 13441-5700

This report has been reviewed by the Rome Laboratory Public Affairs Office (PA) and is releasable to the National Technical Information Service (NTIS). At NTIS it will be releasable to the general public, including foreign nations.

RL-TR-92-218 has been reviewed and is approved for publication.

APPROVED:

PETER D. GIANINO
Project Engineer

FOR THE COMMANDER:

HAROLD ROTH, Director
Solid State Sciences
Electromagnetics & Reliability Directorate

If your address has changed or if you wish to be removed from the Rome Laboratory mailing list, or if the addressee is no longer employed by your organization, please notify RL(EROP) Hanscom AFB MA 01731-5000. This will assist us in maintaining a current mailing list.

Do not return copies of this report unless contractual obligations or notices on a specific document require that it be returned.

REPORT DOCUMENTATION PAGE

Form Approved
OMB No. 0704-0188

Public reporting burden for this collection of information is estimated to average 1 hour per response, including the time for reviewing instructions, searching existing data sources, gathering and maintaining the data needed, and completing and reviewing the collection of information. Send comments regarding this burden estimate or any other aspect of this collection of information, including suggestions for reducing this burden, to Washington Headquarters Services, Directorate for information Operations and Reports, 1215 Jefferson Davis Highway, Suite 1204, Arlington, VA 22202-4302, and to the Office of Management and Budget, Paperwork Reduction Project (0704-0188), Washington, DC 20503

1. AGENCY USE ONLY (Leave Blank)

2. REPORT DATE
August 1992

3. REPORT TYPE AND DATES COVERED
Final Jun 91 - Jun 92

4. TITLE AND SUBTITLE
AN OPTICAL CONSENSUS CORRELATOR FOR CLUTTERED TARGETS

5. FUNDING NUMBERS
C - F19628-91-C-0106
PE - 61102F
PR - 2305
TA - J7
WU - 41

6. AUTHOR(S)
Dr. Roger S. Putnam

7. PERFORMING ORGANIZATION NAME(S) AND ADDRESS(ES)
Aerodyne Research Inc.
45 Manning Road
Billerica MA 01821

8. PERFORMING ORGANIZATION REPORT NUMBER
ARI-RR-934

9. SPONSORING/MONITORING AGENCY NAME(S) AND ADDRESS(ES)
Rome Laboratory (EROP)
Hanscom AFB MA 01731-5000

10. SPONSORING/MONITORING AGENCY REPORT NUMBER
RL-TR-92-218

11. SUPPLEMENTARY NOTES
Rome Laboratory Project Engineer: Peter D. Gianino/EROP/(617) 377-5119

12a. DISTRIBUTION/AVAILABILITY STATEMENT
Approved for public release; distribution unlimited.

12b. DISTRIBUTION CODE

13. ABSTRACT (Maximum 200 words)
The phase-only Consensus Correlator improves the probability of detection of targets obscured by other objects such as a stand of trees. The technique involves masking out most of the input scene and using a standard correlator to search for small pieces of the expected target shape. The areas of the input scene that are found to contain pieces of the target are combined in a final correlation. The Consensus Correlator reduces the transfer of noise that is interspersed with pieces of the target in the input scene to the vicinity of the correlation spike in the correlation plane. A preliminary investigation of an appropriate figure of merit for comparing correlation spikes produced by different inputs and phase-only filters is also presented.

14. SUBJECT TERMS
Pattern recognition, target detection, optical correlation, phase-only filter, clutter, Fourier plane filter

15. NUMBER OF PAGES
48

16. PRICE CODE

17. SECURITY CLASSIFICATION OF REPORT	18. SECURITY CLASSIFICATION OF THIS PAGE	19. SECURITY CLASSIFICATION OF ABSTRACT	20. LIMITATION OF ABSTRACT
UNCLASSIFIED	UNCLASSIFIED	UNCLASSIFIED	UL

1.0 ABSTRACT

A need exists for optical target recognition in the presence of clutter. Our innovation has been demonstrated to improve the signal-to-background ratio of the target correlation spike by masking off most of the cluttered input scene to reduce the background noise. The correlation process is repeated for each small section of the input scene to find the visible pieces of the target, and is then repeated one final time with the mask passing all the sections of the input scene which were found to have pieces of the target but without the surrounding clutter.

The significance here is found in the fact that for heavily cluttered targets a higher correlation spike-to-background ratio is obtained by reducing the size of the input scene, even if visible parts of the target are left out. This occurs because the input scene is mostly background clutter with a few separated pieces of visible target. This Consensus Filter mimics the human capacity to detect targets in heavily cluttered scenes by concentrating on small sections and ignoring the surrounding areas. It also overcomes the poor repeatability of a human who is working on large amounts of input data. The new requirement of having to repeat the correlation for each piece of the input scene simply better utilizes the extreme speed of the optical correlator. The tradeoff that this new technique entails is the need to evaluate the large number of spikes, each of which indicates a possible piece of the target.

The demonstration involves a military scout car as a target shape. The target is mostly obscured, leaving only small portions visible. The obscured areas are replaced by noise and the Consensus Filter is applied to the whole input scene. The computer model of the optical system breaks the input scene into blocks of 4 x 4 pixels, 8 x 8, 16 x 16, and 32 x 32 pixels. We observed that the Consensus Filter generally has a higher probability of detection than a standard correlator for highly obscured targets. In addition the ratio of the correlation spike to the next largest spike is always larger using the consensus filter because of the reduction in noise background and in some cases by identifying a more optimum fourier plane filter.

Further results for phase-only filters includes the effects of continuously changing the amplitude information in the fourier plane filter from the matched filter condition to the phase-only condition, and beyond to a "hyper" phase-only filter. This sequence continuously increases the performance in terms of the ratio of the main correlation spike to the secondary spike.

In addition a study was undertaken to find an acceptable quality measure of a correlation plane to be used internally by the Consensus Filter. One measure is (max-mean)/mean. The mean and standard deviation of this measure were studied as a function of the target size that was used to create the phase-only filters, and this measure was successfully utilized in the Consensus Filter. Further work is needed on a figure of merit to make the Consensus Filter a fully self contained alternative to the standard correlator.

Other results of this research include comparisons of matched filters and phase-only filters for partially obscured targets, and for random target shapes.

Availability Codes
Dist | Avail and/or Special
A-1
DTIC QUALITY INSPECTED 4

2.0 TABLE OF CONTENTS

3.0 INTRODUCTION

There is a need for target recognition in the presence of clutter. Optical correlation has the advantage of achieving great speed through the parallel nature of the optical fourier transform, and is well adapted to the Consensus Filter which requires a large number of optical correlations.

Our version of the clutter problem is attempting to recognize a target which is partially obscured, say by a stand of trees, but which is otherwise undistorted.

3.1 Description of Results

The demonstration of the Consensus Filter was accomplished by computer simulation of the optical correlator, including the obscured input target, the fourier plane filter, and the ancillary processing based on data taken from the correlation plane. The software programs were written by the principal investigator using Matlab which is a matrix manipulation language, and were run on personal computers using 8086, 80386, and 80486 microprocessors.

The results of this work are that the Consensus Filter concept does better succeed at finding pieces of the target than an ordinary correlator when most of the target is missing. An ordinary correlator is superior when most or all of the target image is available. In addition the Consensus Filter is significantly more complex and will require additional development to optimize its internal decision making for a wider class of target, clutter, and noise scenarios.

An essential component to the operation of the Consensus Filter which involves comparing target correlation spikes from different output correlation planes is a universal figure of merit. This issue was investigated and partially solved, permitting a proper demonstration of the Consensus Filter. This work is discussed in Section 5.

The general issues of phase-only or partially phase-only filters were partially investigated with a focus on the Consensus Filter application. An interesting viewpoint emerged from a series of tests reported in Section 6 which shows that phase-only filter acts more strongly than a matched filter to spectrally "whiten" the input target and therefore produce a correlation spike that better resembles an impulse. This target whitening is extended using a "hyper" phase-only filter which does have amplitude components and produces a correlation spike which is the closest match possible to a perfect impulse.

3.2 Review of the Consensus Correlation Concept

The Consensus Correlator operates by chopping the input scene into pieces which are individually checked by a standard optical correlator which is looking for the whole target. The blocks of the input scene which are found to contain pieces of the target are checked to be sure that their correlation spikes are close together, which ensures that the various target pieces that have been found would fit together properly.

The essential element here is that the size of the chopped up blocks from the input scene which are individually handled by the optical correlator must be smaller than the perfect target shape which was used to create the fourier plane filter. This condition results in the background level of the correlation plane being reduced in the vicinity of the correlation spike. The Consensus Correlator is based on the idea that only a small portion of the target is present and that cutting back on the noise or clutter near this small target piece will give a cleaner correlation spike. The relevance of the target size can be understood from the convolution viewpoint where noise and clutter are spread a distance in the correlation plane equal to the width and height of the target shape. (This is approximately true also for typical phase-only filters.) For example consider the input scene cut into blocks which are 100 times smaller in area than that of the target. The correlation plane receives the uncorrelated (noise) optical power spread out by a factor of 100. If the correlation spike is unchanged, the signal to background ratio in the vicinity of the correlation spike will be 100 times greater.

The improvement in the signal to background ratio occurs because the fourier plane filter spreads out the noise or clutter from the small piece of the input scene. If the masked off block of the input scene is too small then the correlation spike will also be reduced, because the small piece of the target which is visible in the input will also be cut up.

The preference for cutting the input scene into blocks roughly equal to the size of the expected target pieces is accommodated by running the system with several different block sizes and choosing the strongest performer. Our demonstration used 4 x 4 pixels, 8 x 8, 16 x 16, and 32 x 32 pixels. We observe, as expected, better performance when the input is chopped into blocks closest to the size of the target pieces used in the input scene to the correlator.

4.0 CONSENSUS CORRELATOR DEMONSTRATION

We have successfully demonstrated the Optical Consensus Correlator by computer simulation. This demonstration consists of properly locating a highly obscured target with a higher probability than is obtained by using a traditional optical correlator. The origin of the target shape is a military scout car shown in Figure 1. The target is represented as zeros and ones on a 32 x 32 matrix, as shown in Figure 2. The actual input image used is produced by masking off all but a few pieces of the target matrix, and replacing the masked areas by noise, which represents clutter.

The noisy pixels are statistically independent and are generated as the absolute value of a Guassian distributed zero mean process with standard deviation equal to 2 for the maximum clutter level considered. Note that input to the correlator is in terms of electric field and the correlation plane is dealt with in optical power. Finally, the graphs showing the probability of detection versus noise level range in noise level from 0 to 10; 10 representing a noise standard deviation of 2 for the electric field input, and a 1 representing a noise standard deviation of 0.2 for the electric field input. The optical noise or clutter power increases as the square of the number given on the x-axes.

The Consensus Correlator uses a scanning mask to restrict the area being evaluated in the input scene. Four different mask aperture sizes are used, and the target detection probability is given for each one in the graphical data: 4 x 4 pixels blocks, 8 x 8, 16 x 16, and 32 x 32 which gives the response of the standard correlator for comparison.

4.1 The Consensus Correlator Algorithm

This section is a block description of the algorithm used to demonstrate the Consensus Filter, which is reproduced in full in the Appendix.

4.1.1 Scanning the Input Scene: scan2.m

The input scene is a matrix which is first masked off except for a small block as shown in Figure 3, step 1. The masked off input matrix is fourier transformed and then (array) multiplied by

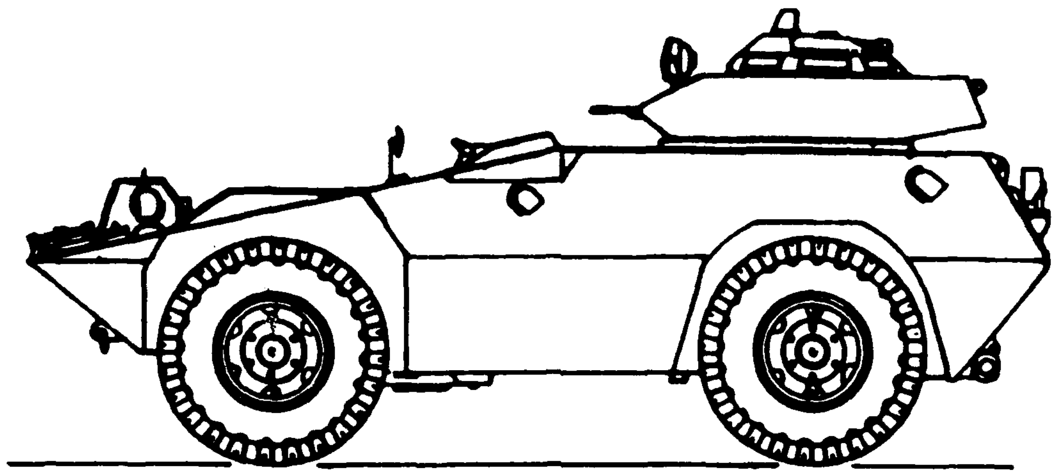

Figure 1. The Cadillac Gage Commando Scout vehicle is used as the target model

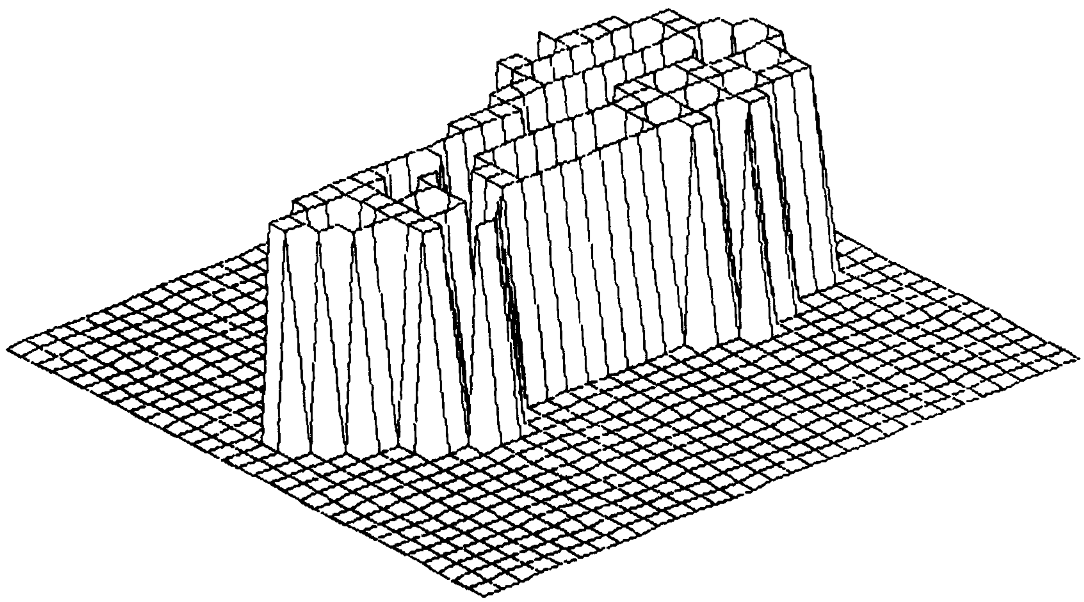

Figure 2. A 3-d image of the 32 x 32 matrix containing the actual target shape using pixels of values zero and one.

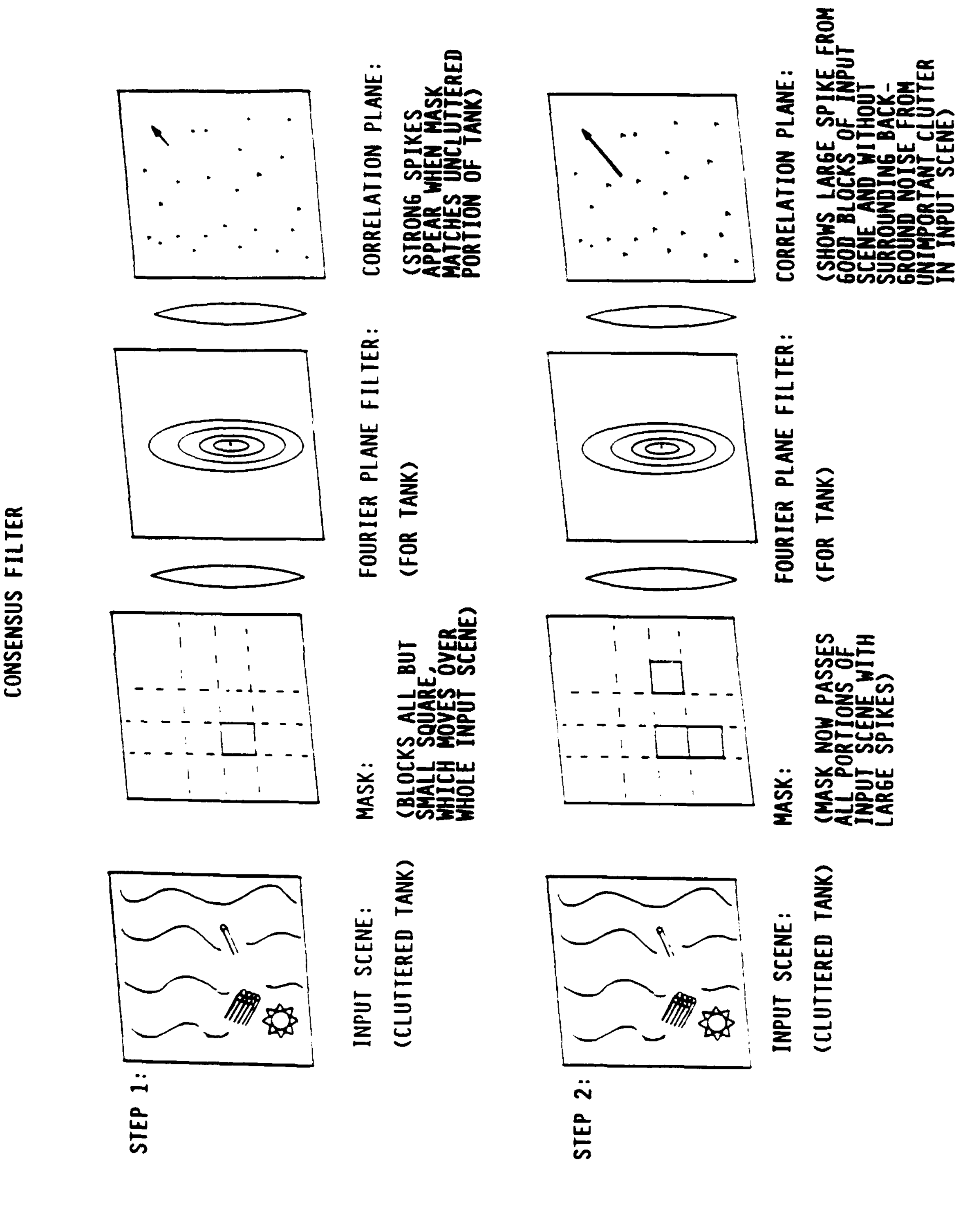
CONSENSUS FILTER
STEP 1:
INPUT SCENE:
(CLUTTERED TANK)
MASK:
(BLOCKS ALL BUT
SMALL SQUARE,
WHICH MOVES OVER
WHOLE INPUT SCENE)
FOURIER PLANE FILTER:
(FOR TANK)
CORRELATION PLANE:
(STRONG SPIKES
APPEAR WHEN MASK
MATCHES UNCLUTTERED
PORTION OF TANK)
STEP 2:
INPUT SCENE:
(CLUTTERED TANK)
MASK:
(MASK NOW PASSES
ALL PORTIONS OF
INPUT SCENE WITH
LARGE SPIKES)
FOURIER PLANE FILTER:
(FOR TANK)
CORRELATION PLANE:
(SHOWS LARGE SPIKE FROM
GOOD BLOCKS OF INPUT
SCENE AND WITHOUT
SURROUNDING BACK-
GROUND NOISE FROM
UNIMPORTANT CLUTTER
IN INPUT SCENE)

Figure 3.

the phase-only target filter, inverse transformed, absolute valued and squared to produce the correlation plane. The largest spike is noted and other spikes are noted if they are above a certain threshold fraction of the largest spike (software variable : ff). The maximum number of spikes accepted is limited (variable : spkbx). The location of these spikes is recorded. This analysis is repeated for the entire input scene using one piece of the input scene at a time.

4.1.2 Grouping the Correlation Spikes: test3.m

The purpose here is to determine if there is any overlap of the correlation spikes from the various sections of the input scene. An overlap suggests that the correlation spikes were produced by various parts of a target that would fit together properly. The algorithm hunts for closely located correlation spikes, with an adjustable maximum separation (variable : space).

4.1.3 Final Mask Comparison: finmask2.m

This step creates a new mask which is placed in front of the input scene and passes only those blocks of the input scene which had individually produced a correlation spike at a common location. See Figure 3, step 2. This masked input is fed to the correlator and the resulting correlation spike is located and measured. Running the correlator on an input scene where only those parts of the scene that have pieces of the target are passed will result in a much larger correlation spike and a minimum of noise or clutter.

A further improvement occurs at this point. A phase-only filter is not optimum for a partially obscured target; and this is discussed at greater length in Section 6. A new phase-only fourier plane filter is produced based on the apparent location of the target (correlation spike) and the implied parts of the target found in the input scene. (This uses optfilt2.m.) This new optimized phase-only filter is applied to the masked input and the new correlation spike observed. This optimization procedure is then repeated a second time. This phase-only fourier plane filter which is optimized to match the visible pieces of the target can noticeably sharpen the resulting correlation spike.

During the process of reconstructing a more closely matched fourier plane filter, the mask is also checked to be sure it doesn't pass any parts of the input scene where, based on the new knowledge of the target location, there could not be any target components.

This whole process is repeated for the other likely mask combinations which were indicated by groups of overlapping correlation spikes from the first scan of the input scene. The single optimized correlation spikes resulting from the resulting mask combinations are compared and one target location is selected. The figure of merit used to make this comparison is discussed in Section 5.

The algorithm is designed to reduce transmission of clutter from the input scene to the immediate vicinity of the detection spike in the correlation plane. This concept is also presented by Figures 3 and 4.

4.2 Four Examples of Cluttered Target Detection

4.2.1 Two Small Pieces of Target Visible

Figure 5 shows a contour of the target shape with two 4 x 4 pixel boxes drawn in to indicate the two small pieces of the target that will be visible at the input of the correlator. The remainder of the matrix has noise added. Figure 6 compares the probability of detection of the standard correlator (solid line) with the Consensus Correlator (4 x 4 blocks are dash-dot, 8 x 8 are dot-dot. 16 x 16 are dash-dash) as a function of increasing background noise. The performance of the 4 x 4 pixel mask used to scan the input scene gives the best performance as is expected since it is a good match with the size of the visible pieces of the target. The probability of detection is obtained by running ten different versions of the noise.

Figure 7 shows the average ratio of the correlation spike to the secondary peak for the four cases, with zeros averaged in if the target was not correctly located. The Consensus Correlator both reduces the noise and clutter in the correlation plane and optimizes the detection filter, which is shown to improve the ratio of the correlation spike to the secondary peak: ratio = (max-median)/(2nd max-median).

4.2.2 One Small Piece of Target Visible

Figure 8 presents the target with an emphasized box which shows the only visible part of the target with noise everywhere else in the input matrix. Figure 9 shows the probability of

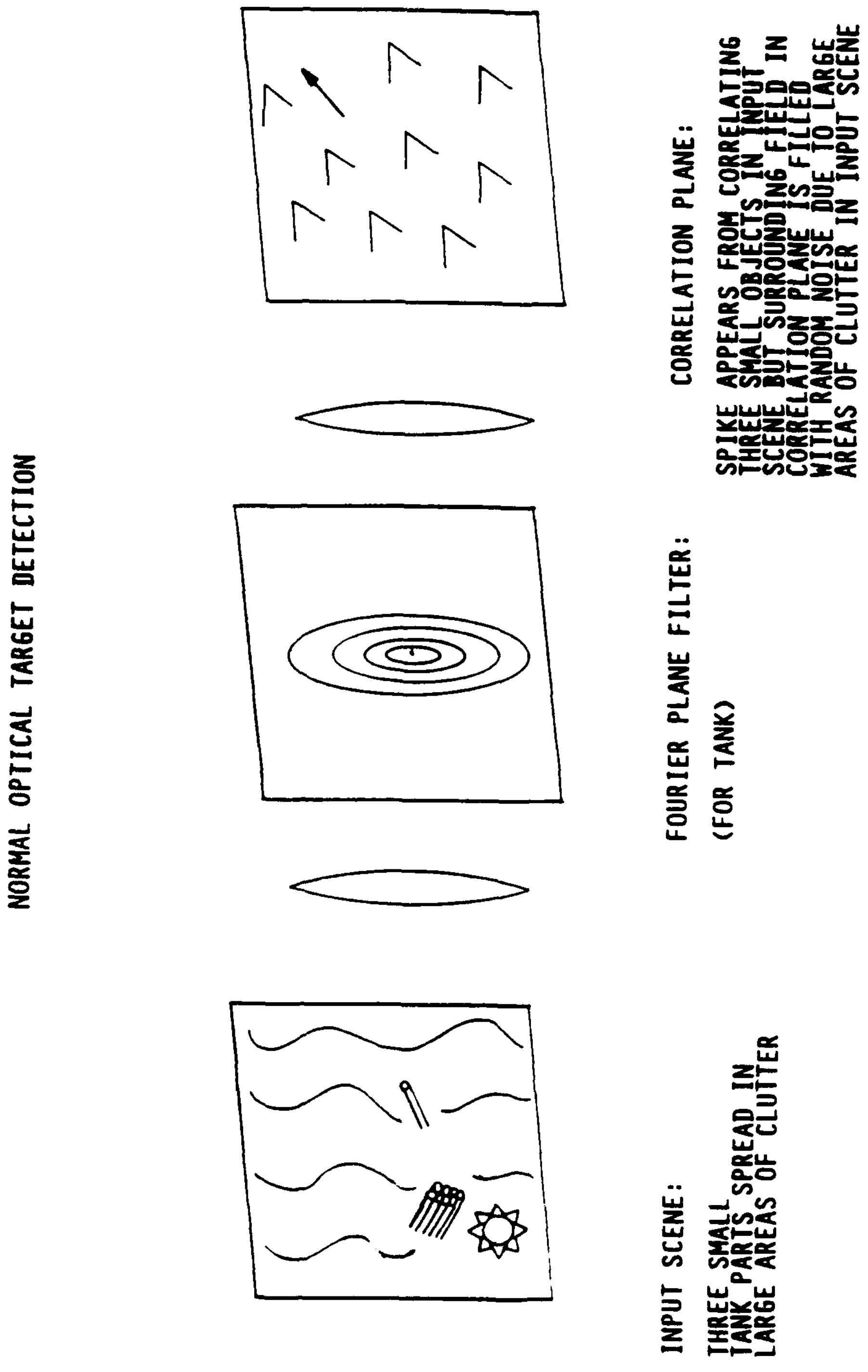
NORMAL OPTICAL TARGET DETECTION
INPUT SCENE:
THREE SMALL
TANK PARTS SPREAD IN
LARGE AREAS OF CLUTTER
FOURIER PLANE FILTER:
(FOR TANK)
CORRELATION PLANE:
SPIKE APPEARS FROM CORRELATING
THREE SMALL OBJECTS IN INPUT
SCENE BUT SURROUNDING FIELD IN
CORRELATION PLANE IS FILLED
WITH RANDOM NOISE DUE TO LARGE
AREAS OF CLUTTER IN INPUT SCENE

Figure 4.

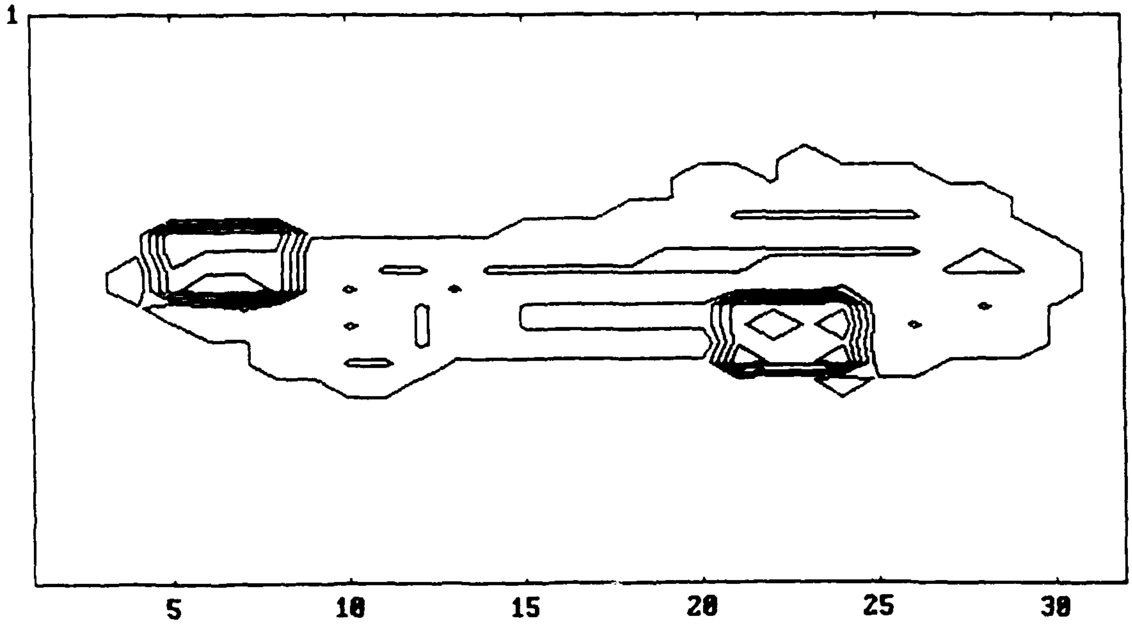

Figure 5. A contour of the target shape with two 4 x 4 pixel boxes to emphasize the two small pieces of the target that are presented to the input of the Consensus Correlator.

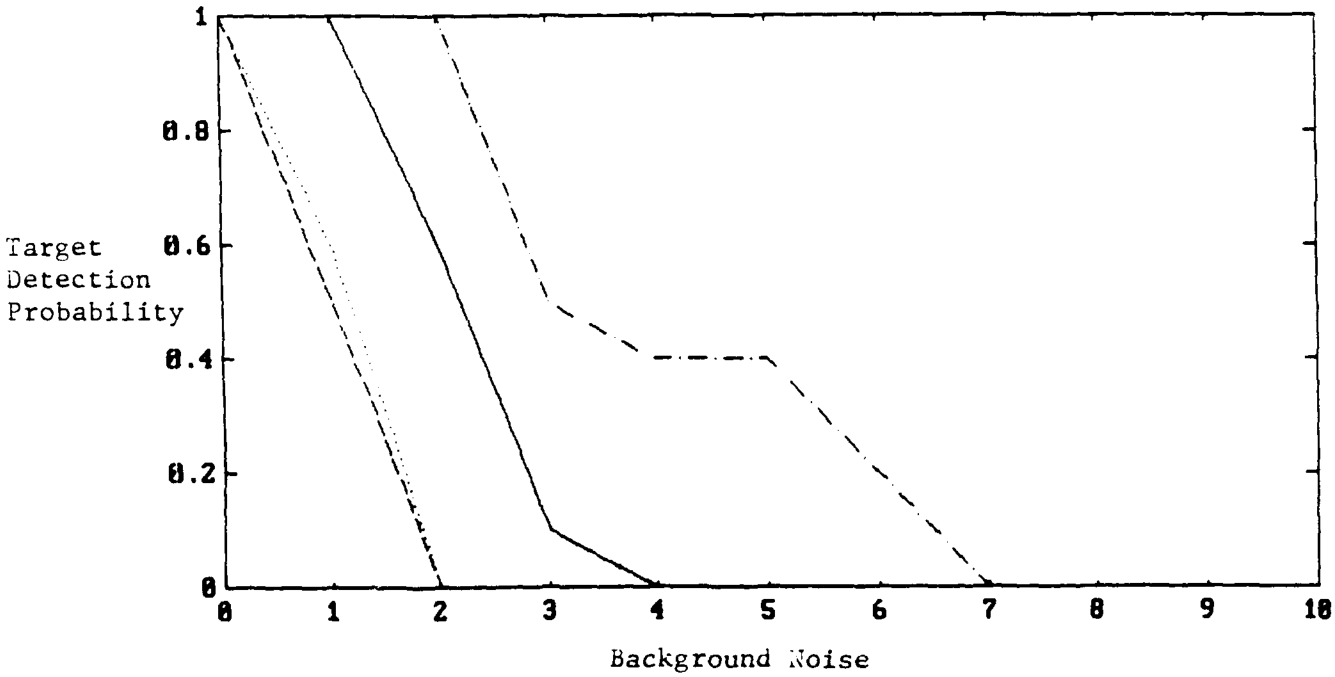

Figure 6. The probability of target detection shows the expected decrease with increasing noise level. The background optical noise rises as the square of the x-axis values of 0-10. The solid line is the standard correlator. The scanning 16 x 16 pixel box is dash-dash, the 8 x 8 is dot-dot, and the 4 x 4 is dash-dot. The 4 x 4 mask shows performance superior to the standard correlator. This is based on ten runs using different noise inputs.

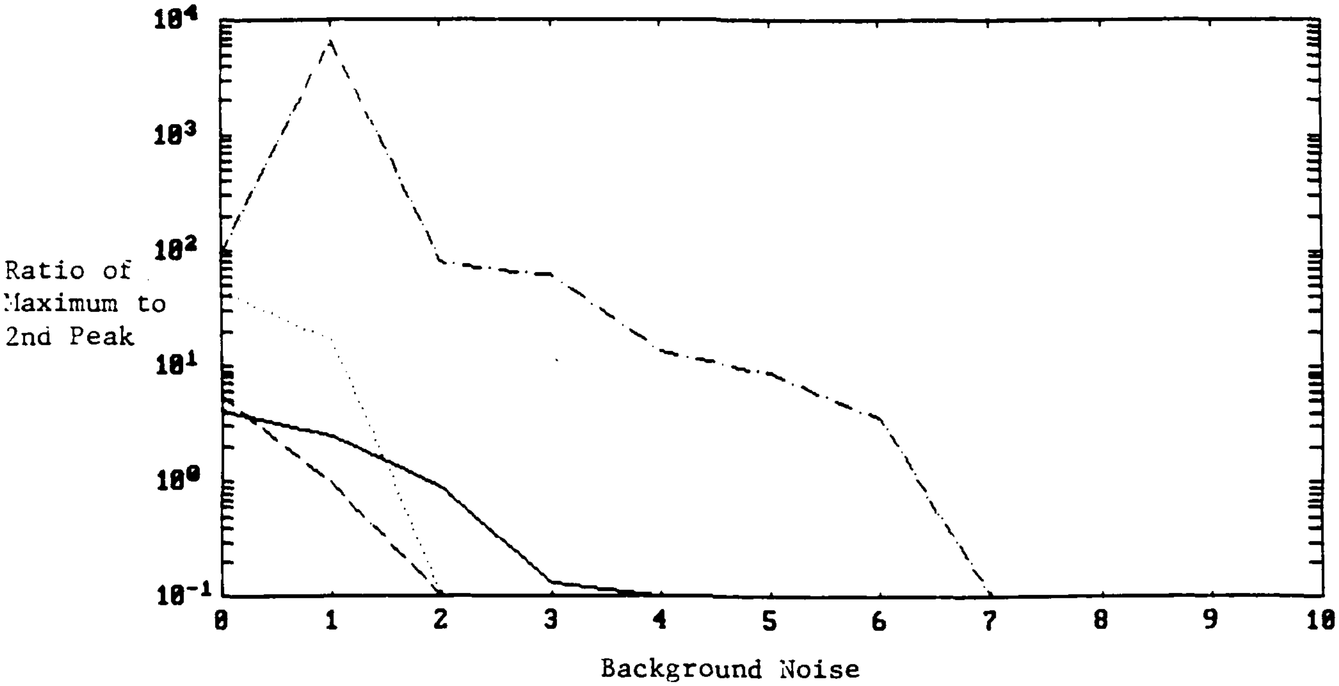

Figure 7. The ratio of the amplitude of the primary correlation spike to the amplitude of the secondary peak shows an advantage of the Consensus Correlator in reducing background noise. The dash-dot curve is the 4 x 4 pixel mask and the solid curve is the standard correlator. The horizontal axis is the background noise level.

detection as a function of noise and clutter with the 4 x 4 mask (dash-dot) giving the best result. Again, a 4 x 4 mask is a good match with the size of the visible target piece. The 16 x 16 mask system failed even at low noise which, due to a few similar failures elsewhere, is assumed to be a software problem.

4.2.3 <u>One 8 x 8 Pixel Piece of the Target Visible</u>

Figure 10 shows the target shape with an 8 x 8 pixel box emphasizing the small fraction of the target shape which is visible. The remaining area of the input scene is filled with noise. Figure 11 shows the probability of detection as a function of noise and clutter intensity. The 8 x 8 pixel mask (dot-dot) gives the best performance, and it is the best match for the size of the visible target piece.

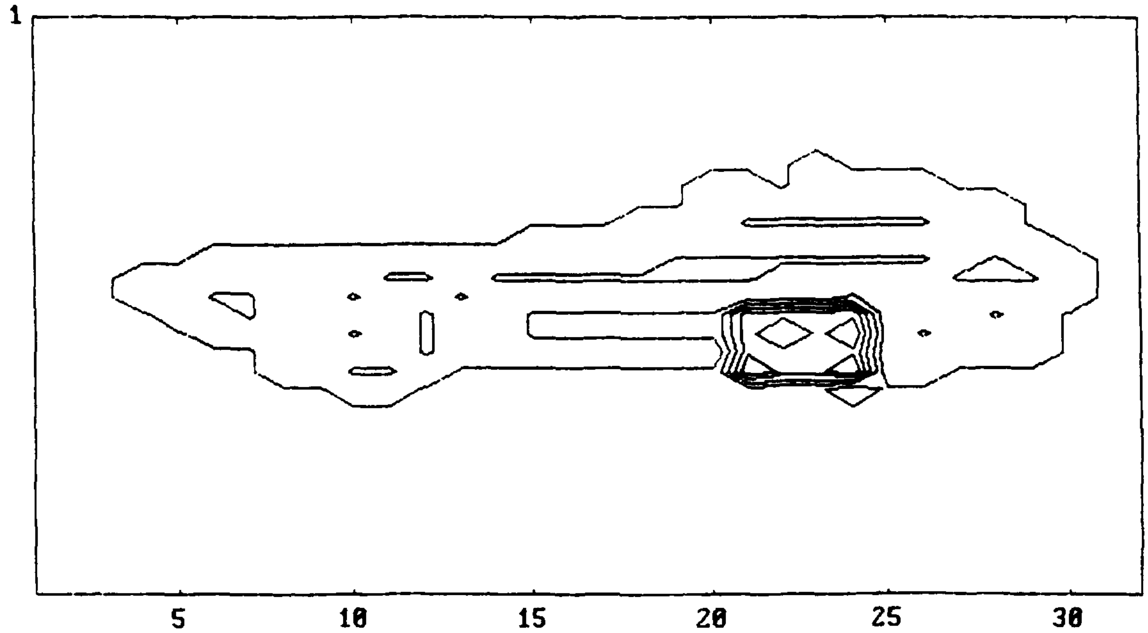

Figure 8. The emphasized 4 x 4 pixel box shows the smaller portion of the target shape used as the input for Section 4.2.2.

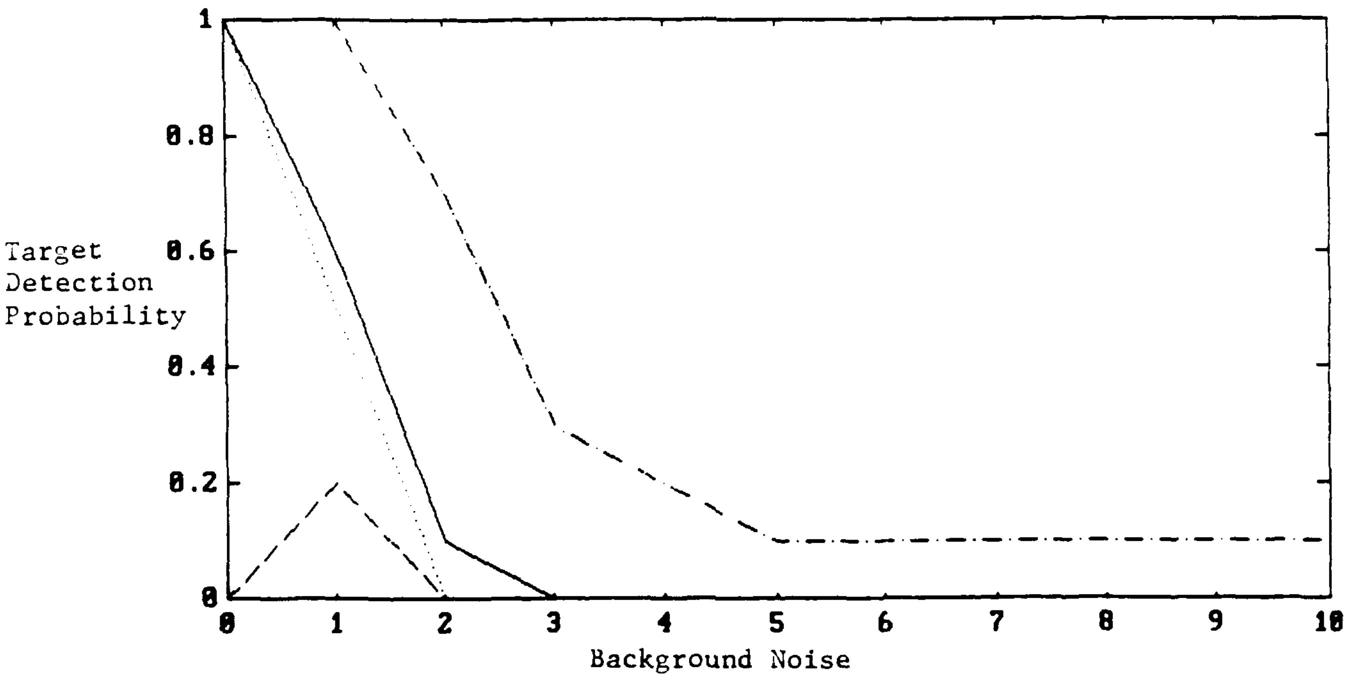

Figure 9. Probability of target detection versus noise level for the previous figure. The 4 x 4 pixel scanning mask (dash-dot) is superior to the standard correlator.

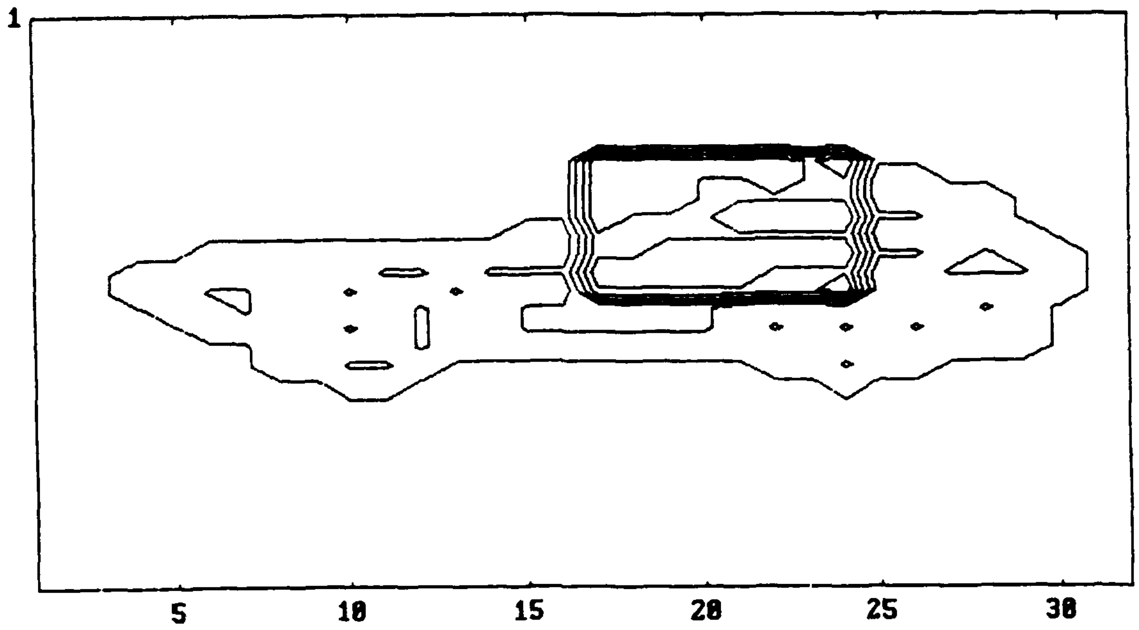

Figure 10. The emphasized 8 x 8 pixel box shows the portion of the target shape used as the input for Section 4.2.3.

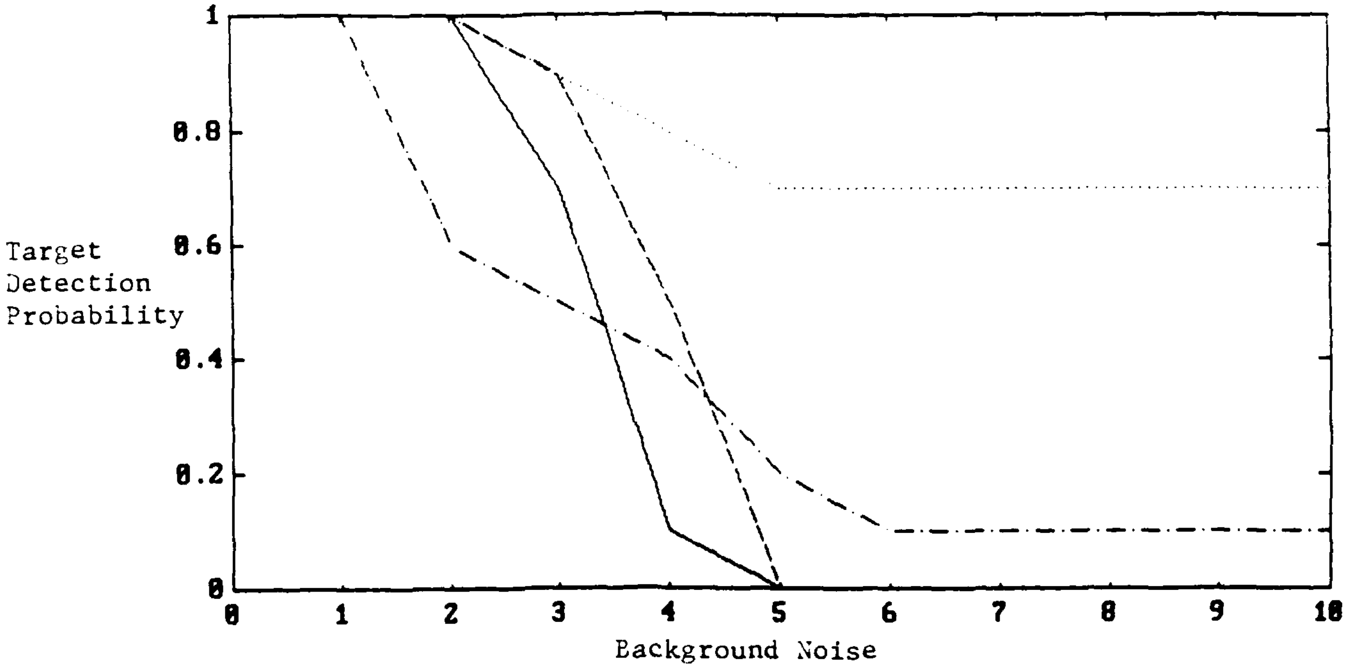

Figure 11. Probability of target detection versus noise level for the previous figure. The 8 x 8 pixel scanning mask (dot-dot) is superior to the standard correlator.

4.2.4 One 8 x 8 Pixel Piece of the Target Visible with a Shift in the Target Position

Figure 12 shows the target shape with an 8 x 8 pixel box denoting the fraction of the target shape that is visible. In addition a shift in the position of the target was arranged to highlight the sensitivity of the Consensus Correlator to fortuitous overlaps of the scanning mask and any visible piece of the target. The algorithm has not yet been modified to desensitize it to this condition. Figure 13 shows the probability of detection versus noise and clutter. In this case the 4 x 4 pixel mask (dot-dash) is superior to the 8 x 8 mask (dot-dot) despite the 8 x 8's better size match. The 8 x 8 mask apparently accepts excessive noise in comparison to the 4 x 4 mask due to a weak overlap in the mask scanning step.

The Consensus Correlator demonstrates a superiority over the standard correlator when a small fraction of the expected target is visible.

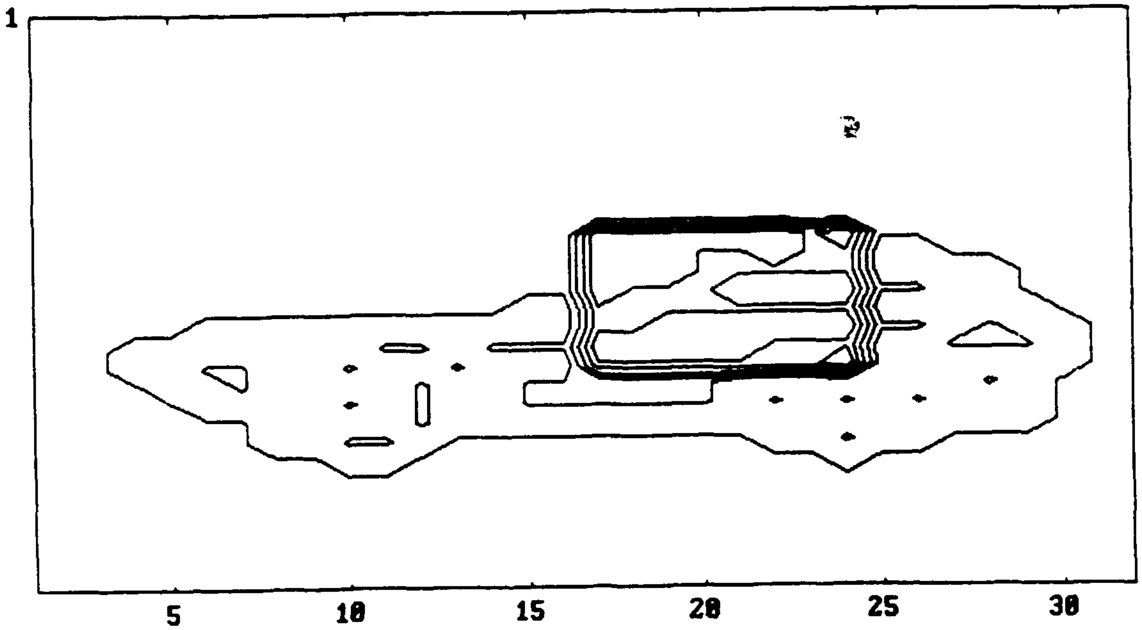

Figure 12. The emphasized 8 x 8 pixel box shows the portion of the spatially shifted target shape used as the input for Section 4.2.4.

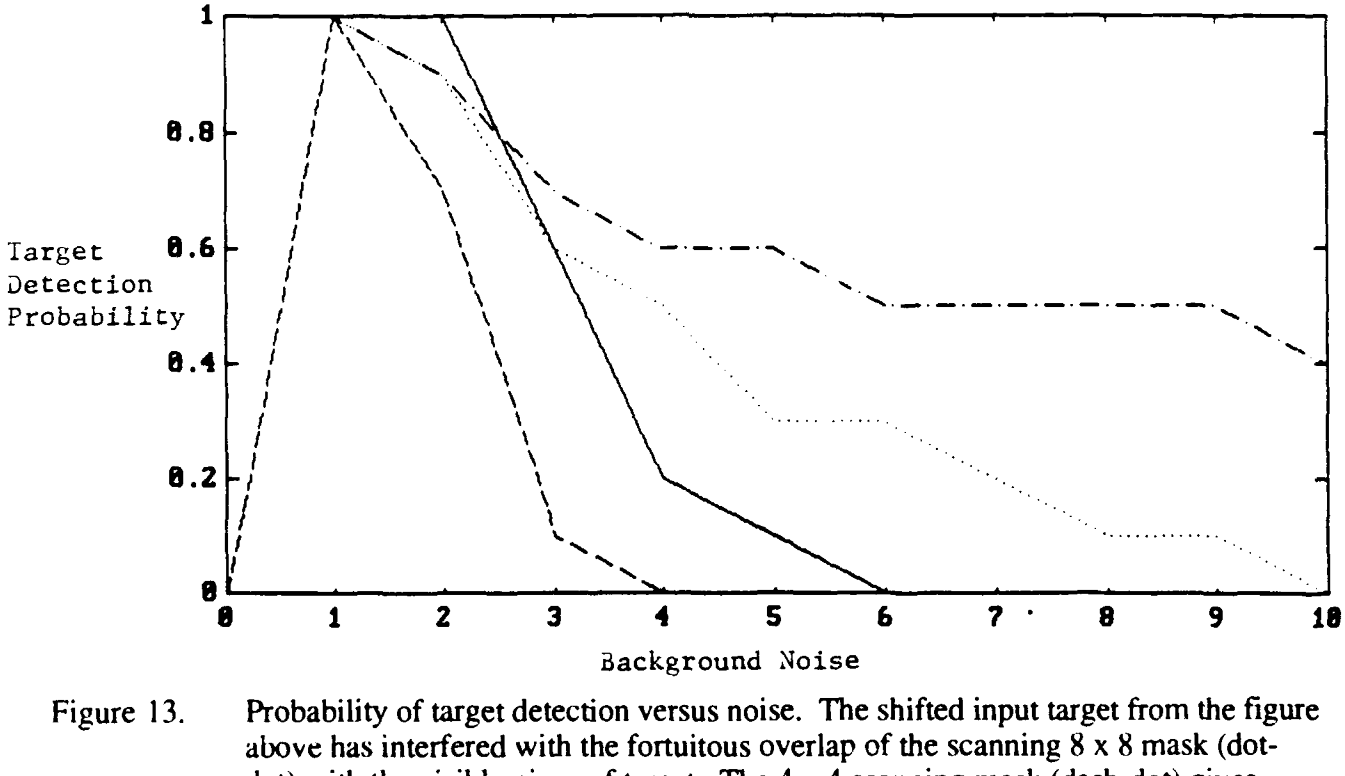

Figure 13. Probability of target detection versus noise. The shifted input target from the figure above has interfered with the fortuitous overlap of the scanning 8 x 8 mask (dot-dot) with the visible piece of target. The 4 x 4 scanning mask (dash-dot) gives superior performance.

5.0 FIGURE OF MERIT FOR THE CORRELATION PLANE PRODUCED BY A PHASE-ONLY FILTER

One of the steps in the Consensus Correlator Algorithm involves comparing correlation spikes among cases where different amounts of the input scene are masked off as well as having used different phase-only filters. This clarifies the need for a robust figure of merit. One figure of merit that was tested was the ratio of the correlation spike height to the secondary peak (after subtracting the background). This is an important measure but our implementation did not give consistent results. A second measure which showed some consistency is: (max-mean)/mean. The next two subsections present our preliminary work on this latter figure of merit.

5.1 Target Size Effects in Matched Filter and Phase-Only Filter Correlators

To assess the effect of the number of pixels in a target shape on matched filter and phase-only filter correlators, a test using target shapes with 1 to 1024 nonzero pixels was designed (using a 32 x 32 matrix). The target shapes use pixels with values zero or one, and these are randomly located. In this test a new fourier plane filter that was made to match each random target was then correlated with its target. The resulting correlation peak, mean, (peak-mean) and the (peak-mean)/mean are graphed in Figures 14 and 15 as a function of the number of pixels in the random targets.

The Consensus Correlator is designed to handle the situation where smaller numbers of pixels are available, which suggests that we examine the left edge of the eight graphs of Figures 14 and 15 for constant behavior. We observe that (max-mean)/mean is the most constant, but only for phase-only correlators. This result tentatively supports the (max-mean)/mean formula as a reasonable figure of merit.

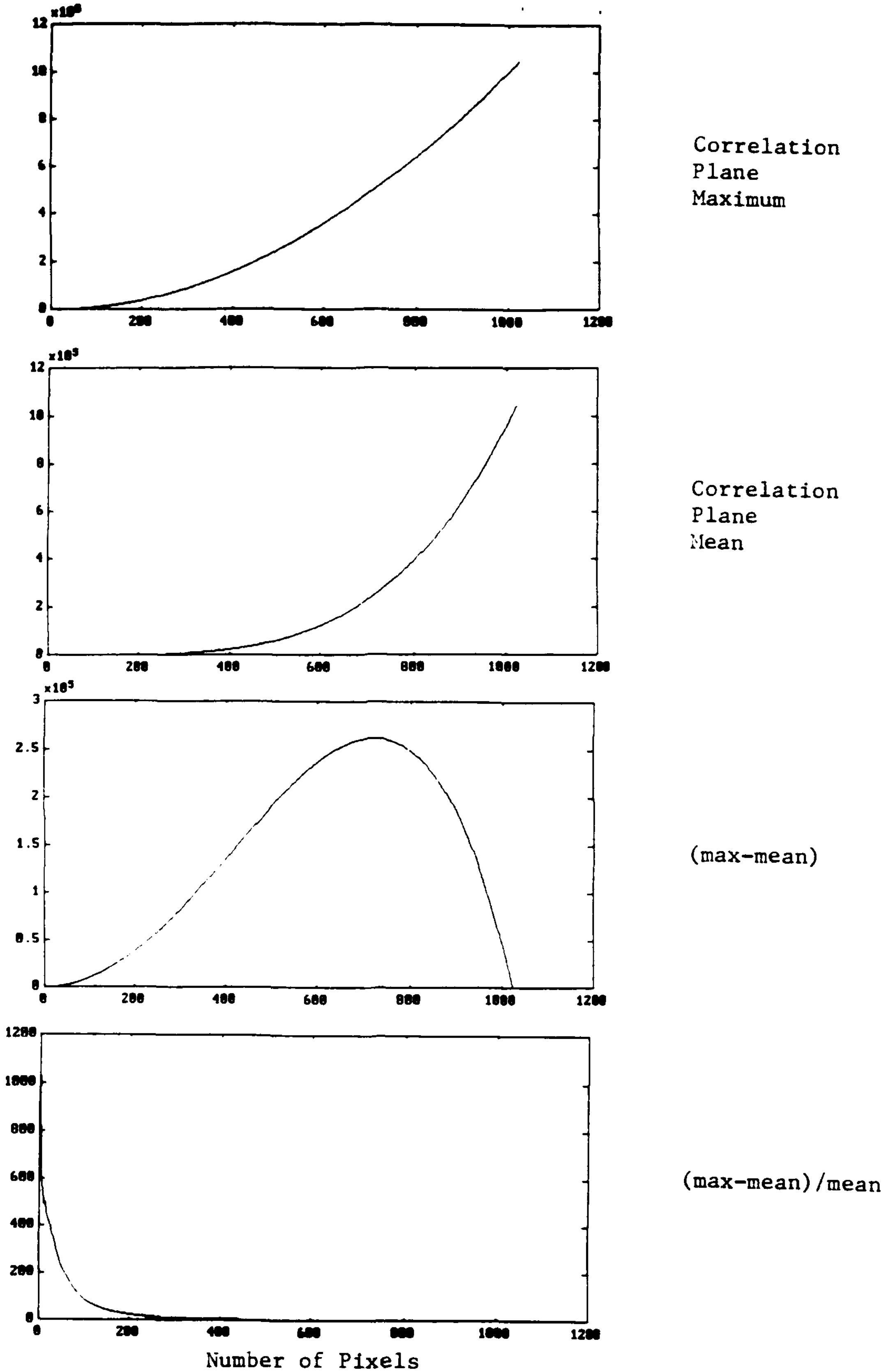

Figure 14. The four graphs measure the performance of a 2-d correlator where the input is a random pattern of ones and zeros and the fourier plane filter is the corresponding MATCHED FILTER. The horizontal axis is the number of pixels that are ones. The graphs beginning at the top of the page are: the correlation plane maximum, mean, (max-mean), and (max-mean)/mean.

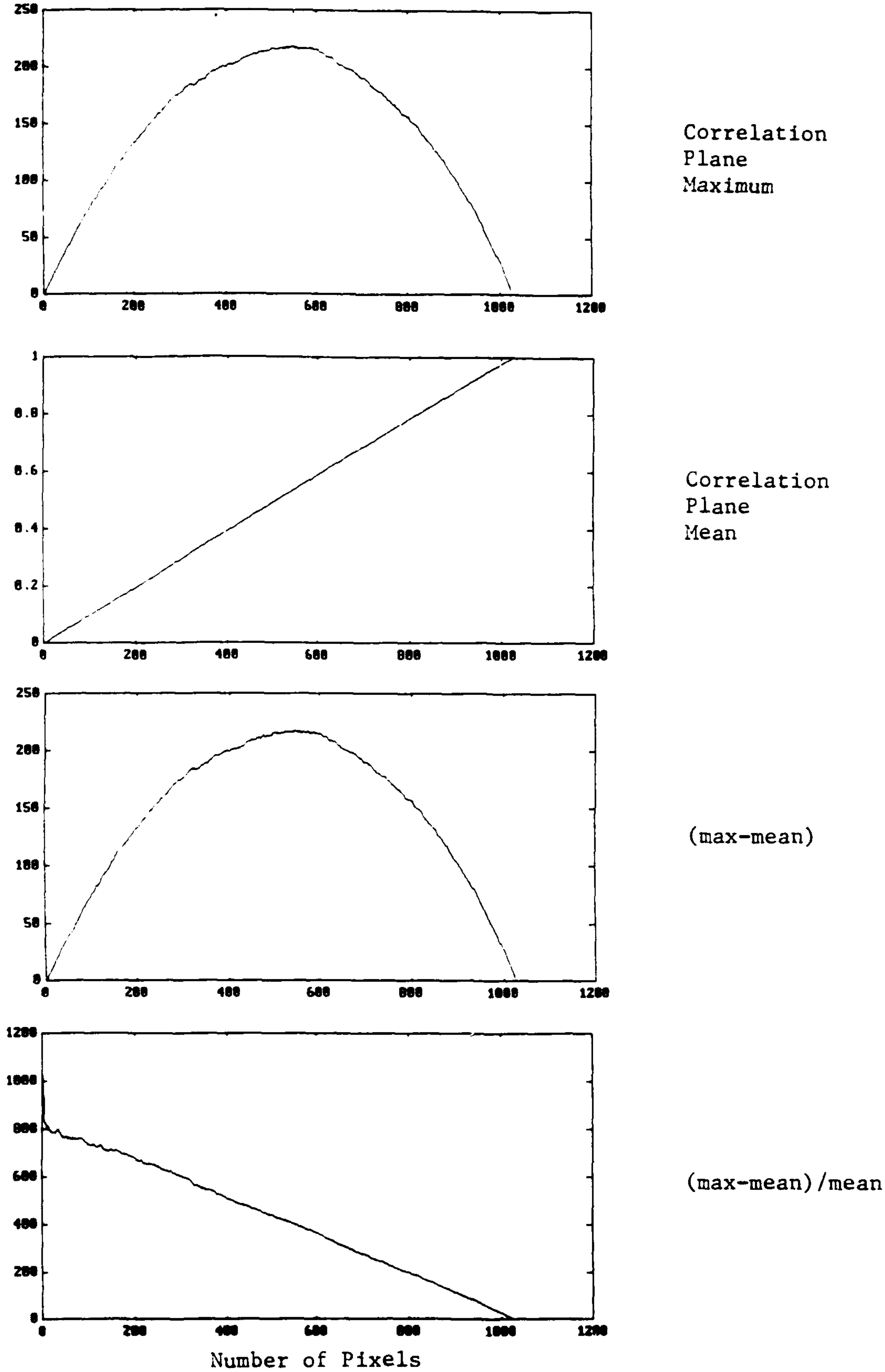

Figure 15. The four graphs measure the performance of a 2-d correlator where the input is a random pattern of ones and zeros and the fourier plane filter is the corresponding PHASE-ONLY FILTER. The horizontal axis is the number of pixels that are one's. The graphs beginning at the top of the page are: the correlation plane maximum, mean, (max-mean), and (max-mean)/mean.

5.2 Correlation Plane Statistics for Uncorrelated Noise Inputs as a Function of the Size of the Expected Target

An evaluation of the behavior of the measure (max-mean)/mean for real target filters but with pure unrelated noise as the input is necessary. This is important because it provides a more absolute measure of the significance of a given correlation spike.

This was investigated by using a random noise input (absolute value of Gaussian noise) and a phase-only correlator whose filter is derived from a real target shape. This real target shape was based on our standard car target but with a variable number of pixels, starting with just one column of pixels at the left and increasing the number of pixels by including progressively more columns stepwise to the right.

Figures 16 and 17 show the mean and standard deviation of the measure [(max-mean)/mean] as a function of the number of pixels in the basis target of the phase-only filter, using 512 different input noise fields. The dashed lines are the data and the solid lines are a simple exponential model.

The data in these two subsections suggests that the measure (max-mean)/man is somewhat insensitive to the number of pixels in the basis target for target detection and follows a predictable course for noise inputs. The figure of merit tentatively adopted for (max-mean)/mean was the number of standard deviations above the noise norm of [(max-mean)/mean].

This figure of merit was used in the algorithm with reasonable success. However the effects of the thresholding decisions, the larger number of cases occuring with the 4 x 4 pixel mask over that of the 16 x 16 pixel masks, and the regenerative optimization used on the fourier plane filter have changed the statistics and made the simple figure of merit inadequate for a real system.

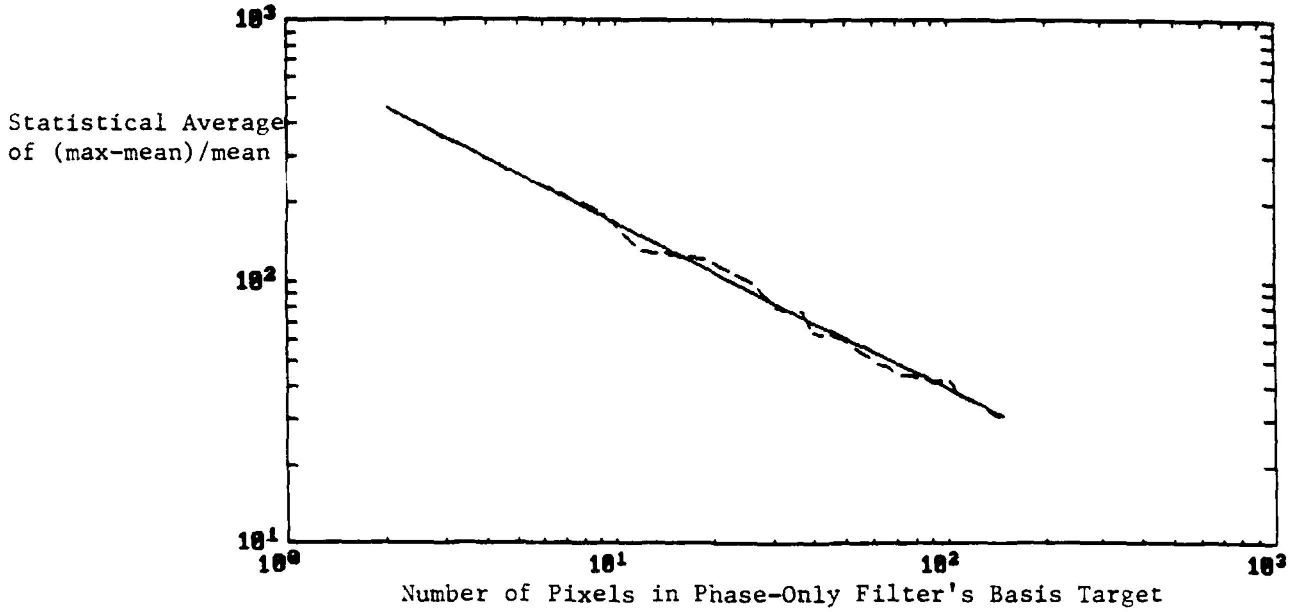

Figure 16. Correlating a phase-only filter which was designed to detect a piece of a known target (scout car) with an unrelated noise field shows that the 512 case average value (vertical axis) of [(max-mean)/mean] of the correlation plane decreases as the number of pixels (horizontal axis) increases in the intended target shape.

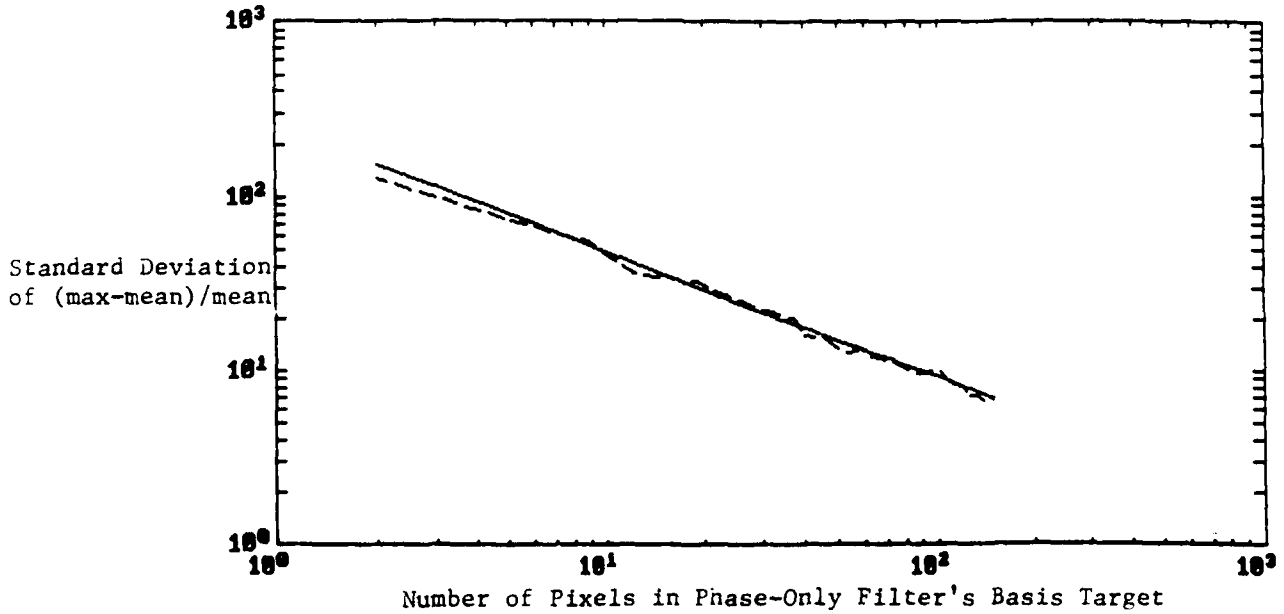

Figure 17. This gives the standard deviation (vertical axis) of [(max-mean)/mean] of the correlation plane versus the number of pixels in the intended target which is used to create the phase-only filter. The input is uncorrelated noise.

6.0 A COMPARISON OF MATCHED FILTERS, PHASE-ONLY FILTERS AND HYPER PHASE-ONLY FILTERS

The unusual situation of our Consensus Correlation where most of the target shape is missing suggests we review the relative merits of the phase-only filter and the standard matched filter.

6.1 A Comparison of a Matched Filter and a Phase-Only Filter for Detecting a Small Piece of the Expected Target

A simple test was performed using our standard target to generate a matched filter and a phase-only filter. The input image to the correlator was a masked off version of the target shape, passing only a 4 x 4 pixel area of the target. Figure 18 shows the correlation plane using the matched filter. There are three peaks of equal height. This means that the masked off version of the target shape found 3 locations with the original target shape that gave 100% correlation.

Figure 19 shows the correlation plane of the same masked target but using a phase-only filter. It has two "incorrect" spikes which are twice as large as the spike which correctly locates the target. We observe then that a phase only filter can have erratic behavior for highly masked targets. This is one of the reasons that we arranged for the phase-only filter in the Consensus Correlator Algorithm to be recalculated to better match the visible pieces of the target.

6.2 Spectral Whitening of the Input Target Gives the Sharpest Correlation Spike

This subsection presents a series of correlation planes obtained using the car target with a sequence of fourier plane filters ranging smoothly from a matched filter to a phase-only filter and further into the realm of hyper phase-only filters.

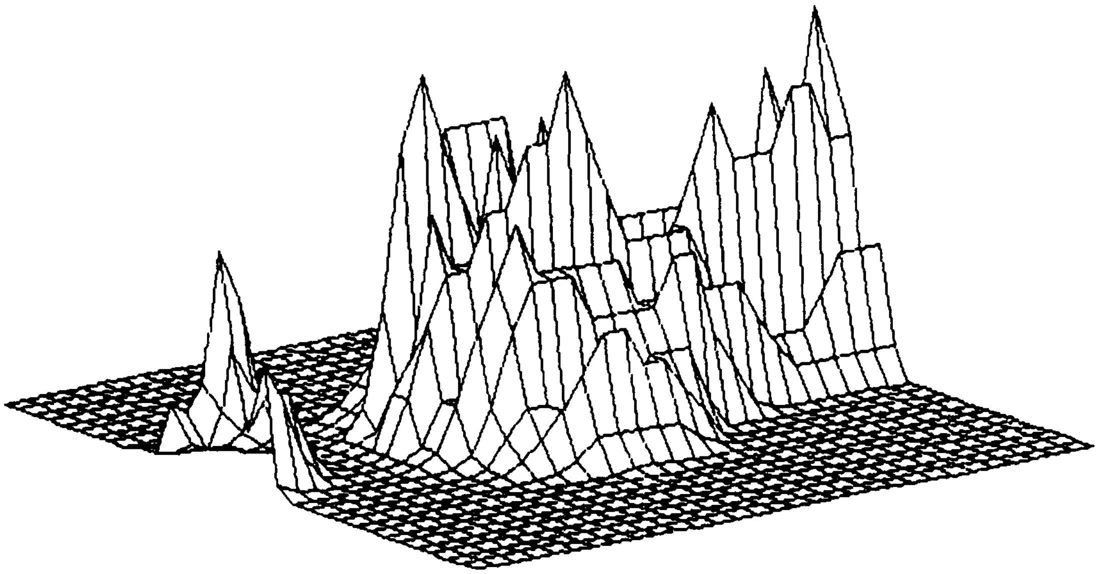

Figure 18. The correlation plane for a 4 x 4 pixel piece of the scout car target as the input and a matched filter based on the whole target in the fourier plane. Three spikes of equal amplitude appear.

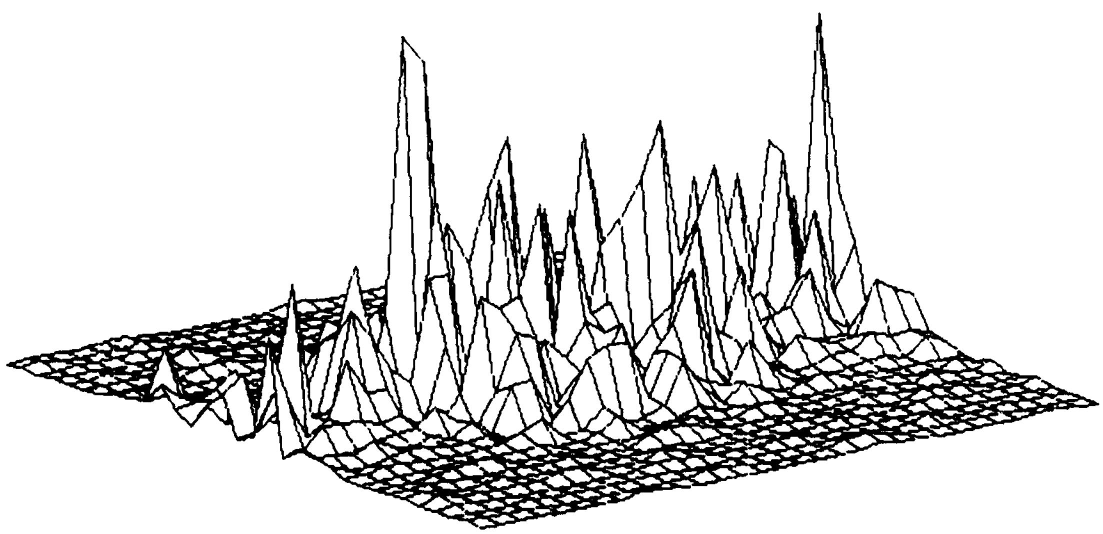

Figure 19. The correlation plane for the same 4 x 4 pixel piece of the scout car used in the previous figure. Here a phase-only filter based on the whole target shape gives two spikes twice as large as the actual correct correlation spike.

Denoting a complex array mf for matched filter, we create a phase-only filter : pof = mf/[ε+|mf|] where ε prevents dividing by zero and we understand that this is an element by element array division. This can be generalized to a general filter: gf = mf/[ε+|mf|]^{exp}. For exp = 0 we create a matched filter. For exp = 1 we create a phase-only filter. For exp = 2 we create a hyper phase-only filter; which is actually not a phase-only filter since it has amplitude information.

Figures 20 and 21 show a sequence of correlation planes beginning with a matched filter (exp = 0) and smoothly changing with exp = 0, .25, .50, .75. 1.0, and 2.0. The correlation spikes get sharper as the exponent approaches 2.0. The exponent exp = 2 has the effect of whitening the spectrum of the target input, all spatial frequencies that are nonzero now have the same amplitude. This extreme adjustment should also have remarkably bad noise properties. However in the complete absence of noise the ratio of the correlation spike height to the secondary peak can achieve very large values. Figure 22 shows the correlation spike height to secondary peak for the car target as a function of the exponent discussed above. The matched filter corresponds to exp = 0; the phase-only filter has exp = 1 and the fully whitened target spectrum has exp = 2.

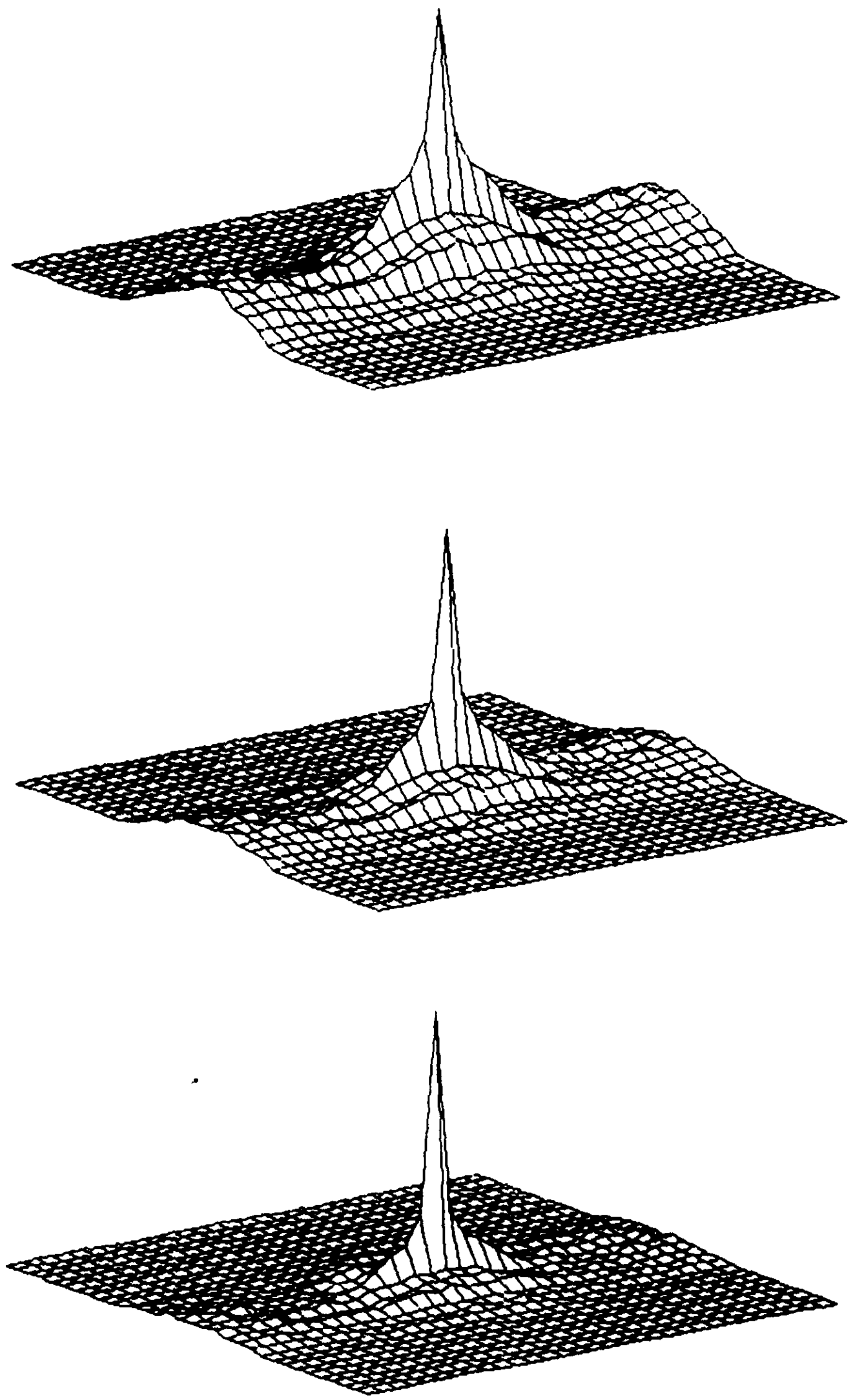

Figure 20. The top correlation plane is the result of the scout car as input and a matched filter. The matched filter has exp = 0 in $gf = mf/[\varepsilon + |mf|]^{exp}$. The middle correlation plane uses exp = .25, and the lower correlation plane uses exp = .50. A phase-only filter would have exp = 1.

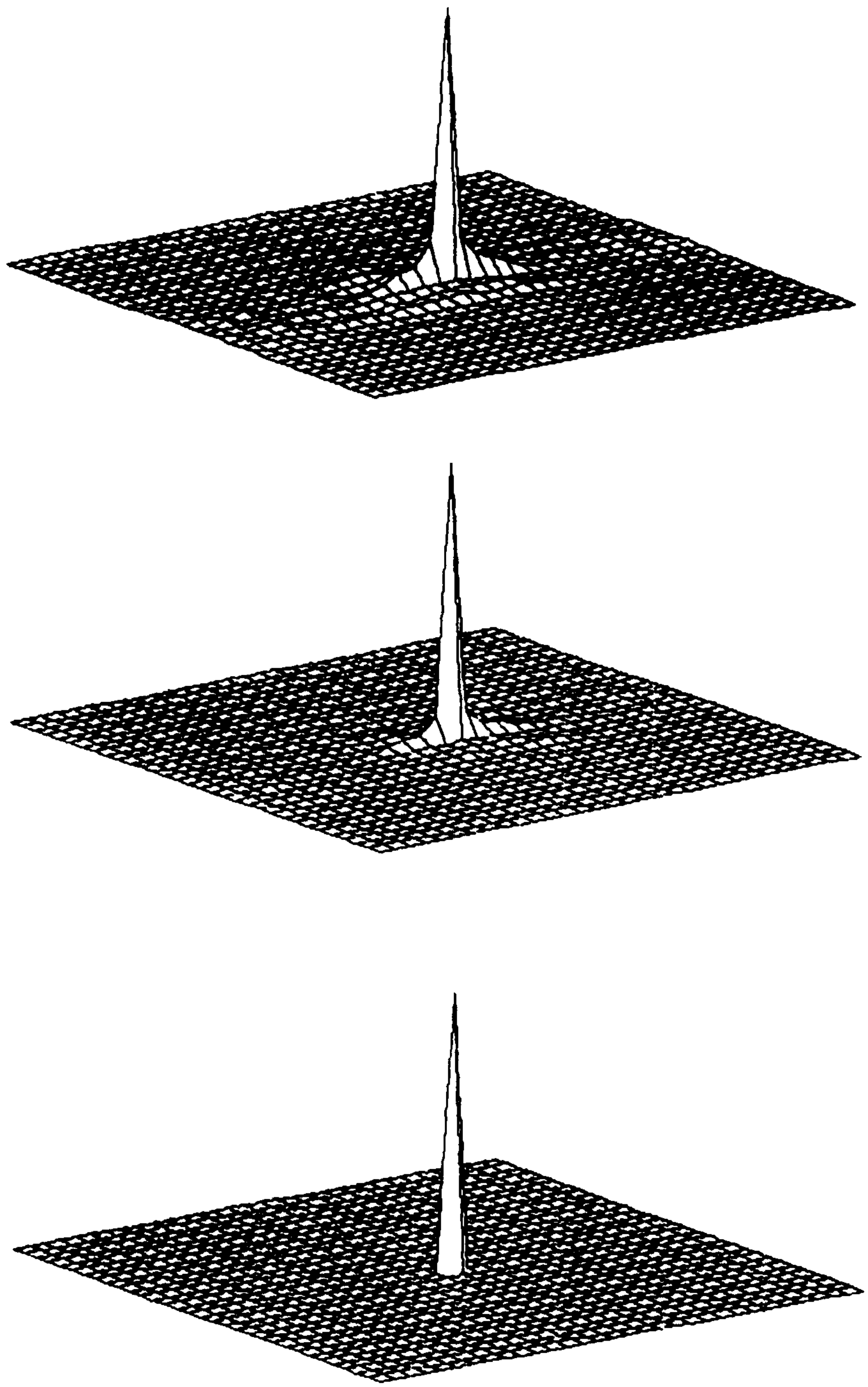

Figure 21. Continuing the correlation results from the previous figure with exp = .75 at the top, exp = 1.0 (phase-only filter) in the middle, and exp = 2.0 at the bottom. The input target spectra is "whitened" when exp = 2, giving a very sharp correlation spike.

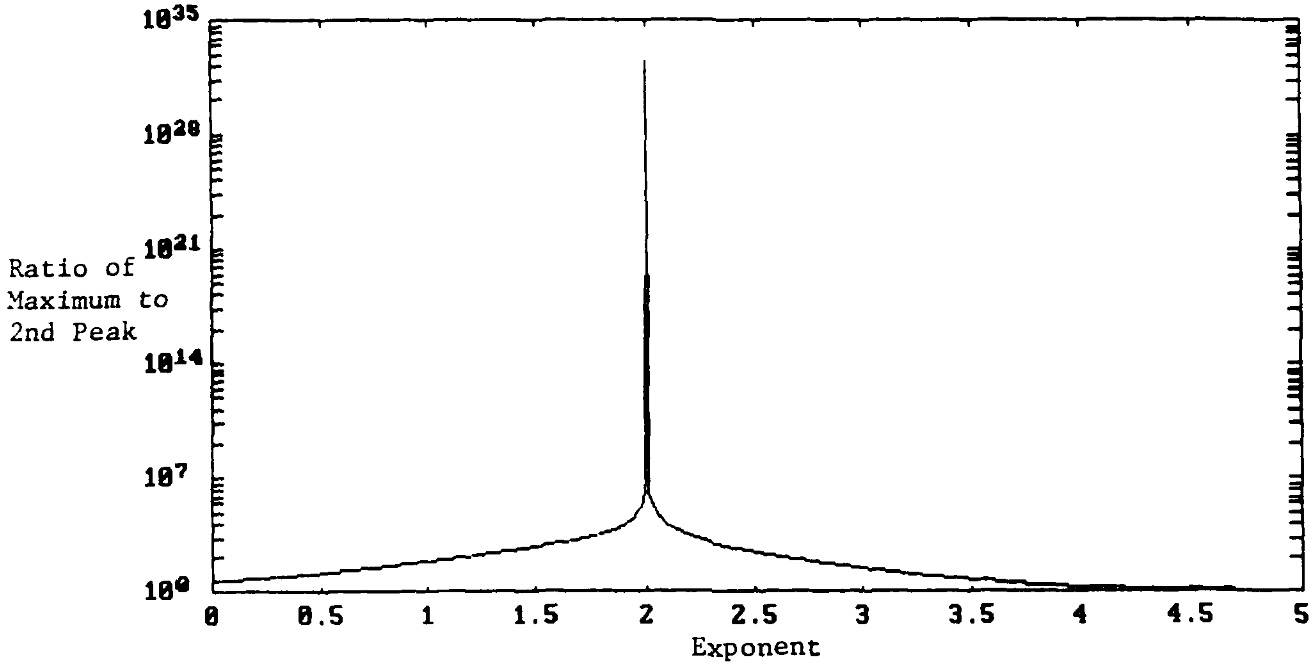

Figure 22. The ratio of the correlation spike height to the secondary peak is shown versus exp (see Figures 20 and 21). At the left with exp = 0 is the matched filter, exp = 1 is a phase-only filter, and exp = 2 uses the fourier plane filter to whiten the input target spectrum resulting in an impulse-like spike in the correlation plane.

7.0 CONCLUSIONS AND RECOMMENDATIONS

We have successfully demonstrated the Consensus Correlator for detecting targets that are mostly obscured. The Consensus Filter mimics the human capacity to notice pieces of a target and to associate them together to determine if they could be part of a single target shape, while ignoring the interspersed clutter. This demonstration used random noise as the background. We recommend that the second demonstration be on targets that are mostly obscured and have a camouflage background consisting of randomly situated pieces of the actual target. The Consensus Correlator will have the advantage here of removing those camouflage pieces which are not situated properly to compose a real target.

The demonstration involved a complicated computer program which we expect would have been even more successful had it been optimized. A portion of the work focused on testing figures of merit which is a central issue for complex optical correlators. Our progress in figures of merit was useful to our own Consensus Correlator demonstration, and additional work in this area would probably receive broad interest from other researchers in this field.

Our demonstration used phase-only filters which facilitated our finding a useful figure of merit but also produced anomalies in the detection of mostly obscured targets. We partially compensated for this behavior by recalculating the phase-only filter using estimates as to what parts of the target were actually present.

Another avenue for increasing our understanding of phase-only filters would be to examine the phase-only filter in the convolution domain: that is, inverse fourier transform a variety of phase-only filters to get experience with their properties in the image domain.

8.0 APPENDIX

The appendix contains a list with a short description of the important functions and script files in Section 8.1. Section 8.2 is a list of the important variables. The program codes developed by the principal investigator are listed in Section 8.3.

8.1 Functions and Script Files

run4.m	Runs whole program
scan2.m:	Moves mask over input scene and collects correlation spikes
test3.m	Groups correlation spikes from all the cases of the masked input scene
finmask2.m	Assembles masks based on groupings of correlation spikes and compares the final performances
optfilt2.m	Calculates a phase-only fourier plane filter optimized for the pieces of the target shape which have been found. Removes parts of mask which cannot overlap with apparent target position.
expand(q)	Expands mask q assuming 32 x 32 matrix (4 x 4 becomes 6 x 6)
peaks(x)	Converts matrix x to matrix with only local maxima (4 nearest neighbors)
optcor(x,y)	Gives correlation plane for input scene x and conjugate fourier plane filter y
msk(a,r,c,bh,bw)	Makes ones in matrix a from (rows) r to r+bh-1 and columns from c to c+bw-1.
plt4(x)	Plots four graphs from matrix with five columns with the x coordinate being the first column and the other four columns being the y's of the four graphs.

8.2 Variables

ms	matrix size, i.e., ms = 32 for a 32 x 32 matrix
bh	box height, i.e., bh = 4 for box height of 4 pixels (chops up input scene)
bw	box width
in	input scene matrix
cfni	conjugate of the 2-D fourier transform filter
thrs1	threshold 1 = minimum spike to secondary ratio for all but largest spike
spkbx	spikes/box = maximum number of correlation plane spikes accepted per chunk of input scene
ff	attenuation of acceptable subsequent spikes below largest spike
rto2	ratio of primary correlation spike to secondary spike (1st-median)/(2nd-median)
rto3	(max-mean)/mean in correlation plane
rfo4	(rto3-eme)/esg
eme	theoretical (estimated) mean value of rto3
esg	theoretical (estimated) standard deviation of rto3
sndpk	second peak value
cpl	correlation plane (matrix)
space	allowable separation of correlation spikes to be considered fitting together into one target

8.3 Software Programs Employing the Matlab Language

```
    %RUN4.M       generates dat3h(bh)ns(ns)=[row,col,rto,bxs,bh,rto2]
%t1=clock;
dat4=[]
dat5=[]
for ns=0:10    %gen dat4 matrix with rto2 and dat5 with rto
 in=car2+(ns*0.2)*gausnoise;     % input noise background
dat4(ns+1,1)=ns;
dat5(ns+1,1)=ns;
 bh=2*ns;
 for div=1:4
  bh=bh/2
  bw=bh;
  scan2
  test3
  finmask2
    if (abs(row-17)<=space & abs(col-17)<=space)
    dat4(ns+1,div+1)=rto2;
%   dat5(ns+1,div+1)=rto;
    dat5(ns+1,div+1)=mxdvfa;
    end
 end
end
save cons7.mat dat4 dat5 space spkbx ff ff2 thrs1
%t2=clock;
```

```
%SCAN2.M
% Generates dat1 using ff,ms,bh,bw,in,cfni,thrs1,spkbx
%t=clock;
dat1=zeros((floor(ms/bh))*spkbx*(floor(ms/bw)),7);
ii=0;
for m=1:floor(ms/bh),
for n=1:floor(ms/bw),
mk=zeros(ms,ms);
mk=msk(mk,1+(m-1)*bh,1+(n-1)*bw,bh,bw);
cpl=optcor(mk.*in,cfni);
mesh(cpl)
me=mean(mean(cpl));
sgm=std(cpl(:));
mxx=max(max(cpl));
rto=(mxx-me)/sgm;
ffrto=ff*rto;
for zz=1:spkbx,
[yy,k]=max(cpl);
[mx,col]=max(yy);
row=k(col);
rto=(mx-me)/sgm;
if (rto<=ffrto),break,end;
cpl(row,col)=0;
ii=ii+1
dat1(ii,1:5)=[m,n,mx-me,row,col];
if (rto<=thrs1),break,end;
end
end
end
dat1=dat1(1:ii,:)
```

```
   %  TEST3.M       Uses dat1 and space (0 to 4) for initial "sep"
%This is a script file version of test2.m and changes dat1
% It finds neighbors for minimum seperation "sep"
[l1,z]=size(dat1);
  for sp=space:5
x=zeros(l1,1);
dat1(:,7)=zeros(l1,1);
for pp=1:l1
x(:,1)=(abs(dat1(pp,4)-dat1(:,4))<=sp & abs(dat1(pp,5)-dat1(:,5))<=sp),
x(:,1)=(x(:,1)==1 & (dat1(pp,1)~=dat1(:,1) | dat1(pp,2)~=dat1(:,2))),
dat1(:,7)=dat1(:,7) + x(:,1);
% bxs=0;              %this section gives number of different boxes that
% w=[-1 -1];          %contain neighboring spikes for each spike
%  for qq=1:l1
%   if (x(qq,1)==1 & (any(dat1(qq,1:2)~=w)))
%   bxs=bxs+1;
%   w=dat1(qq,1:2);
%   end
%  end
% dat1(pp,6)=bxs;
end
sep=sp;
if (max(dat1(:,7))>0),break,end;
end
[mx row]=max(dat1(:,3));
 if dat1(row,7)==0
 dat1(row,7)=1;
 end
for pp=1:l1
 if dat1(pp,7)==0
  dat1(pp,7)=1;
 end
end
```

```
     % FINMASK2.M
%This is a script file that assembles masks and compares them
dat2=dat1(dat1(:,7)>0,:);  %removes rows without neighbors
%dat2=dat1(dat1(:,6)>0,:);    %removes rows without neighbors
%dat2(:,7)=dat2(:,6);
[ll,z]=size(dat2);
   if ll==0
   [mx3,r]=max(dat1(:,3));
   dat2=dat1(r,:);
   ll=1;
   end
hh=floor(ms/bh);
ww=floor(ms/bw);
sx=-2*ones(hh*ww,1);
   x2=zeros(hh*ww,3);
    for m=1:hh
     for n=1:ww
      x2((m-1)*ww+n,1:2)=[m n];
     end
    end
rsp=0;
[mx7,r]=max(dat2(:,7));     %finds max number of neighbors and the first row
 tt=0;
 rp=0;
rpo=0;
rpo3=0;
rpo4=-1000;
mxdvfa=1000*eps;
%while (max(dat2(:,7)))>=0.5*mx7);  % all groups having half as many neighbors
 while (max(dat2(:,7)))>=1 | max(dat2(:,7)))>=0.5*mx7);
 tt=tt+1;
 x=zeros(ll,1);
[mx77,r]=max(dat2(:,7));

 x(:,1)=(abs(dat2(r,4)-dat2(:,4))<=sep & abs(dat2(r,5)-dat2(:,5))<=sep);
 x(:,1)=(x(:,1)==1 & (dat2(r,1)~=dat2(:,1) | dat2(r,2)~=dat2(:,2)));
 smx=sum(x(:,1));
 x(r,1)=1;
  x2(:,3)=zeros(hh*ww,1);
  mx3d=(max(dat2(x,3)))/10;
  for pp=1:ll
   if (x(pp,1)==1 & dat2(pp,3))>=mx3d)
    m=dat2(pp,1);
    n=dat2(pp,2);
    x2((m-1)*ww+n,3)=1;
   end
  end

      if any((x2(:,3)'*sx==sum(sx))&(sum(sx)==sum(x2(:,3))))
       if smx>0
       x(r,1)=smx;
       end
      dat2(r,7)=dat2(r,7)-x(r,1);
      else
      rsp=rsp+1;
      sx(:,rsp)=x2(:,3);
 mk=zeros(ms,ms);
  for sss=1:hh*ww
   if x2(sss,3)==1;
   m=x2(sss,1);
   n=x2(sss,2);
   mk=msk(mk,1+(m-1)*bh,1+(n-1)*bw,bh,bw);  %adds box to mask
   end
```

```
  end

       % contour(mk,1)
 cpl=optcor(mk.*in,cfn1);
       % mesh(cpl)
  if smx>0
  x(r,1)=smx;
  end
 dat2(r,7)=dat2(r,7)-x(r,1);    % reduces neighbor number
 % dat2
 [yy,k]=max(cpl);
 [mx,col]=max(yy');
 row=k(col);
  pts=148;
  if (bh~=32 | bw~=32)
  optfilt2                         % optimizes the mask and filter
  end
       % [row,col]
 fa=(sum(sum(mk)))/(ms^2);       % mask fractional area (noise est.)
me=mean(mean(cpl));
rto3=(mx-me)/me;
eme=717.78*pts.^(-0.63);  %expected value of rto3
esg=255*pts.^(-0.72);     %standard deviation of rto3
rto4=(rto3-eme)/esg;      %num of std above expected value
%  sgm=sqrt(sum(sum(cpl.^2)/(ms^2))-me^2);
%  rto=(mx-me)/sgm;
% if (rto2)rp & mx/(bxs^2))=mxdvbx/25);
%    if (rto)rpo & mx/(bxs^2))=mxdvbx/25);
%   if(rto3)rpo3 & mx>1.0e-30);
  if(rto4)rpo4 & mx)1.0e-30);
%    if (mx-me)/fa)mxdvfa;  % signal to area (noise) estimate
       contour(mk,1)
        pause(2)
 pks=peaks(cpl);
  % mesh(pks)
 pks(row,col)=0;
    row2=-5;
    col2=-5;
     for sk=1:(1+2*space)^2;
     [yy2,k2]=max(pks);
     [mx2,col2]=max(yy2);
     row2=k2(col2);
     if (abs(row-row2))space)|(abs(col-col2))space),break,end;
     pks(row2,col2)=0;
     end
sndpk=max(max(pks));
med=median(median(cpl));
rto2=(mx-med)/(sndpk-med);
% eval(['dat3h',int2str(bh),'ns',int2str(ns),'=[row,col,rto,bxs,bh,rto2]']);
       mesh(cpl)
        pause(2)
       [row,col]
       rto4
%   dat2(r,4:5)
    mxdvfa=(mx-me)/fa;
   rpo3=rto3;
   rpo4=rto4;
   rp=rto2;
    rpo=rto;
   row1=row;
   col1=col;
   end
  end
end
rto2=rp;
row=row1;
col=col1;
rto=rpo;
rto3=rpo3;
rto4=rpo4;
```

```
%  Optfilt2.m is a script file which calculates a phase-only 2-d
%             optical correlation filter which is optimized for
%             the pieces of the target shape which have been found.
%             Uses row,col of correlation spike which is expected
%             at 17,17.  Removes parts of mask that doesn't overlap
%             with detected target location.

mk2=shift(mk,17-row,17-col);
mk2=car2.*expand(mk2);
cfni2=conj(fft2(mk2));
cfni2=cfni2./(eps+abs(cfni2));
mk2=expand(expand(mk2));
cpl=optcor(in.*mk.*shift(mk2,row-17,col-17),cfni2);
[yy,k]=max(cpl);
[mx,col]=max(yy);
row=k(col);

mk2=car2.*shift(mk,17-row,17-col);
cfni2=conj(fft2(mk2));
cfni2=cfni2./(eps+abs(cfni2));
mk2=expand(expand(mk2));
mk=mk.*shift(mk2,row-17,col-17);
cpl=optcor(in.*mk,cfni2);
[yy,k]=max(cpl);
[mx,col]=max(yy);
row=k(col);
```

```
function z=expand(q); %Expands mask in 32,32 matrix (4 by 4 into 6 by 6)
a=zeros(32,32);
a=q + shift(q,-1,0) + shift(q,1,0);
a=a + shift(a,0,-1) + shift(a,0,1);
z=a>0.5;
```

```
%PEAKS converts input matrix to matrix with only local maxima
%       -all others set to zero, including the outer rim
%       (maxima must be greater than or equal 4 nearest neighbors)

function y=peaks(x);

[r,c]=size(x);
a=zeros(r,c);
a(2:r-1,2:c-1)=(x(2:r-1,2:c-1))=x(1:r-2,2:c-1));
b=a;
a(2:r-1,2:c-1)=(x(2:r-1,2:c-1))=x(3:r,2:c-1));
b=b.*a;
a(2:r-1,2:c-1)=(x(2:r-1,2:c-1))=x(2:r-1,1:c-2));
b=b.*a;
a(2:r-1,2:c-1)=(x(2:r-1,2:c-1))=x(2:r-1,3:c));
b=b.*a;
y=b.*x;
```

```
function z=optcor(x,y)
z=(abs(fftshift(ifft2(fft2(x).*(y))))).^2;
```

```
C:\MATLAB\SIGNAL>type msk.m
function z=msk(a,r,c,bh,bw)
a(r:r+bh-1,c:c+bw-1)=ones(bh,bw);
z=a;
```

```
function y=plt4(x)   %plots matrix as four graphs
                     %assuming 5 columns with the
                     %X coordinate being the first
                     %column and the other 4 columns
                     %being the 4 graphs (y's)

                     %pad with zeros
dat=x>0.1;
x(:,2:5)=x(:,2:5).*dat(:,2:5);
dat=dat==0;
x(:,2:5)=x(:,2:5)+0.1*dat(:,2:5);
x1=x(:,1);
y1=x(:,2);
y2=x(:,3);
y3=x(:,4);
y4=x(:,5);
semilogy(x1,y1,x1,y2,'--',x1,y3,':',x1,y4,'-.')
```

U.S. GOVERNMENT PRINTING OFFICE

MISSION

OF

ROME LABORATORY

Rome Laboratory plans and executes an interdisciplinary program in research, development, test, and technology transition in support of Air Force Command, Control, Communications and Intelligence (C^3I) activities for all Air Force platforms. It also executes selected acquisition programs in several areas of expertise. Technical and engineering support within areas of competence is provided to ESD Program Offices (POs) and other ESD elements to perform effective acquisition of C^3I systems. In addition, Rome Laboratory's technology supports other AFSC Product Divisions, the Air Force user community, and other DOD and non-DOD agencies. Rome Laboratory maintains technical competence and research programs in areas including, but not limited to, communications, command and control, battle management, intelligence information processing, computational sciences and software producibility, wide area surveillance/sensors, signal processing, solid state sciences, photonics, electromagnetic technology, superconductivity, and electronic reliability/maintainability and testability.